J|A|C|S
ARTICLES
Published on Web 05/19/2007

Colloid Chemical Reaction Route to the Preparation of Nearly Monodispersed Perylene Nanoparticles: Size-Tunable Synthesis and Three-Dimensional Self-Organization

Longtian Kang,[†,‡] Zhechen Wang,[†,‡] Zongwei Cao,[†,‡] Ying Ma,[†] Hongbing Fu,*[,†] and Jiannian Yao*[,†]

Contribution from the Beijing National Laboratory for Molecular Sciences (BNLMS), Institute of Chemistry, Chinese Academy of Sciences, Beijing 100080, People's Republic of China and Graduate School of the Chinese Academy of Sciences, Beijing 100039, People's Republic of China

Received December 5, 2006; E-mail: jnyao@iccas.ac.cn; hongbing.fu@iccas.ac.cn

Abstract: By employing a colloid chemical reaction method we demonstrate the preparation of organic nanoparticles composed of perylene molecules (PeNPs) based on the reduction of perylene perchlorate by Br^- anions in the presence of cetyl trimethyl ammonium bromide (CTA^+Br^-) in acetonitrile. A discrete nucleation event, followed by a slower controlled growth on the existing particles, is identified during formation of PeNPs. By changing the growth parameters, such as the monomer concentration and the method of injection, quasi-spherical PeNPs with controllable sizes from 25 to 90 nm could be obtained. The homogeneous solution phase of this method makes it capable of large-scale synthesis of PeNPs with a size distribution (<10%) that is improved by formation of a protective layer of CTA^+ around the PeNPs. The three-dimensional, hierarchical self-organization of 25-nm PeNPs building blocks is observed to form nanobelts and square nanorods, possibly templated by the CTA^+ lamellar micelle structures in acetonitrile. Spectroscopic results reveal two kinds of trends in the development of the optical properties of perylene as they evolve from the molecular to the bulk phase in the nanometer range. The so-called size dependence is evidenced by a switch from Y-type to E-type excimers as the size of the PeNPs increased from 25 to 90 nm. As the 25-nm PeNPs organize into nanobelts or square nanorods the oscillator strength of the Y-type excimers is relatively enhanced. That is, collective phenomena develop as the proximal particles interact in the glassy solids. Our very recent results indicate that this colloid chemical reaction method can also be applied to other organic compounds.

Introduction

In recent years organic nanoparticles (ONPs) of low-molecular-weight functional compounds have inspired growing research efforts[1−6] due to their potential use in the fields of optoelectronics,[3,6] nonlinear optics,[7] and photonics.[8] ONPs occupy the intermediate state between isolated molecules and the bulk crystal. It has been demonstrated that not only can the wide panel of physical properties provided by functional compounds be fully exploited, but also these properties can also be modulated by the particle size[3−5] and shape.[6] However, although tailor-made molecules can generally be obtained by organic synthesis, predicting how their properties will be affected by the complex, nanostructured morphology is still very

[†] Chinese Academy of Sciences.
[‡] Graduate School of the Chinese Academy of Sciences.

(1) (a) Kasai, H.; Nalwa, H. S.; Oikawa, H.; Okada, S.; Matsuda, H.; Minami, N.; Kakuta, A.; Ono, K.; Mukoh, A.; Nakanishi, H. *Jpn. J. Appl. Phys.* **1992**, *31*, L1132. (b) Kasai, H.; Kamatani, H.; Okada, S.; Oikawa, H.; Matsuda, H.; Nakanishi, H. *Jpn. J. Appl. Phys.* **1996**, *35*, L221. (c) Nakanishi, H.; Oikawa, H. In *Single Organic Nanoparticles*; Masuhara, H., Nakanishi, H., Kasai, K., Eds.; Springer-Verlag: New York, 2003; Chapter 2, pp 17−31.
(2) Horn, D.; Rieger, J. *Angew. Chem., Int. Ed.* **2001**, *40*, 4331.
(3) (a) An, B. K.; Kwon, S. K.; Jung, S. D.; Park, S. Y. *J. Am. Chem. Soc.* **2002**, *124*, 14410. (b) Lim, S. J.; An, B. K.; Jung, S. D.; Chung, M. A.; Park, S. Y. *Angew. Chem., Int. Ed.* **2004**, *43*, 6346. (c) Hu, J. S.; Guo, Y. G.; Liang, H. P.; Wan, L. J.; Jiang, L. *J. Am. Chem. Soc.* **2005**, *127*, 17090.
(4) (a) Bertorelle, F.; Lavabre, D.; Fery-Forgues, S. *J. Am. Chem. Soc.* **2003**, *125*, 6244. (b) Birla, L.; Bertorelle, F.; Rodrigues, F.; Badre, S.; Pansu, R.; Fery-Forgues, S. *Langmuir* **2006**, *22*, 6256. (c) Bertorelle, F.; Rodrigues, F.; Fery-Forgues, S. *Langmuir* **2006**, *22*, 8523.
(5) (a) Fu, H. B.; Yao, J. N. *J. Am. Chem. Soc.* **2001**, *123*, 1434. (b) Xiao, D. B.; Xi, L.; Yang, W. S.; Fu, H. B.; Shuai, Z. G.; Fang, Y.; Yao, J. N. *J. Am. Chem. Soc.* **2003**, *125*, 6740. (c) Xiao, D. B.; Yang, W. S.; Yao, J. N.; Xi, L.; Yang, X.; Shuai, Z. G. *J. Am. Chem. Soc.* **2004**, *126*, 15439. (d) Fu, H. B.; Loo, B. H.; Xiao, D. B.; Xie, R. M.; Ji, X. H.; Yao, J. N.; Zhang, B. W.; Zhang, L. Q. *Angew. Chem., Int. Ed.* **2002**, *41*, 962.
(6) (a) Balakrishnan, K.; Datar, A.; Oitker, R.; Chen, H.; Zuo, J.; Zang, L. *J. Am. Chem. Soc.* **2005**, *127*, 10496. (b) Balakrishnan, K.; Datar, A.; Naddo, T.; Huang, J.; Oitker, R.; Yen, M.; Zhao, J.; Zang, L. *J. Am. Chem. Soc.* **2006**, *128*, 7390. (c) Datar, A.; Balakrishnan, K.; Yang, X.; Zuo, X.; Huang, J.; Oitker, R.; Yen, M.; Zhao, J.; Tiede, D. M.; Zang, L. *J. Phys. Chem. B* **2006**, *110*, 12327. (d) Fu, H. B.; Xiao, D. B.; Yao, J. N.; Yang, G. Q. *Angew. Chem., Int. Ed.* **2003**, *42*, 2883. (e) Tian, Z. Y.; Chen, Y.; Yang, W. S.; Yao, J. N.; Zhu, L. Y.; Shuai, Z. G. *Angew. Chem., Int. Ed.* **2004**, *43*, 4060.
(7) (a) Kim, S.; Zheng, Q. D.; He, G. S.; Bharali, D. J.; Pudavar, H. E.; Baev, A.; Prasad, P. N. *Adv. Funct. Mater.* **2006**, *16*, 2317. (b) Oikawa, H.; Kasai, H.; Nakanishi, H. In *Anisotropic Organic Materials*; Glaser, R., Kasizynski, P., Eds.; ACS Symposium Series 798; American Chemical Society: Washington, DC, 2002; Chapter 12, pp 169−178.
(8) (a) Peng, A. D.; Xiao, D. B.; Ma, Y.; Yang, W. S.; Yao, J. N. *Adv. Mater.* **2005**, *17*, 2070. (b) Kaneko, Y.; Shimada, S.; Fukuda, T.; Kimura, T.; Yokoi, H.; Matsuda, H.; Onodera, H.; Kasai, H.; Okada, S.; Oikawa, H.; Nakanishi, H. *Adv. Mater.* **2005**, *17*, 160. (c) He, C. B.; Xiao, Y.; Huang, J. C.; Lin, T. T.; Mya, K. Y.; Zhang, X. H. *J. Am. Chem. Soc.* **2004**, *126*, 7792. (d) Wang, F.; Han, M. Y; Mya, K. Y.; Wang, Y.; Lai, Y. H. *J. Am. Chem. Soc.* **2005**, *127*, 10350.

complicated.[9,10] The electronic and optical properties of ONPs are fundamentally different from those of inorganic nanocrystals (NCs)[11] due to weak intermolecular interaction forces of the van der Waals type.[12] Furthermore, the orientation between the building units in inorganic NCs is identical since atoms can be treated as hard spheres; in contrast, the stacking arrangement between organic molecules plays an important role in the properties of ONPs.[13] Uncovering and mapping the structural, electronic, and optical properties of organic compounds as they evolve from the molecular to the bulk phase in the nanometer range requires synthetic routes to prepare a homologous series of monodisperse ONPs. As evidenced by inorganic NCs, sample uniformity facilitates the organization of NCs into close-packed, glassy, and ordered assemblies (known as NC solids) in which new cooperative phenomena develop as the proximal NCs interact.[14] However, hindered by the methods available for the fabrication of ONP arrays, there is an obvious lack of data concerning the nature of the coupling between ONPs as they assembly into close-packed solids.

Approaches to the preparation of ONPs with well-defined structure, however, have been limited by two facts. The first is that ONPs require mild preparation methods because most organic compounds are thermally fragile. The second is that for practical use ONPs must display controllable size and shape, even though the factors that govern these parameters are still poorly understood (relevant to the weak van der Waals intermolecular interactions). Among the few existing methods[1−6,15−19] a simple and still convenient way is the so-called "reprecipitation method".[1−6] In its most widely used variant, a dilute solution of target compound in a water-soluble solvent (i.e., a good solvent) is injected into vigorously stirred water as a poor medium.[1c,3−6] The good solvent disperses, and the sudden change in the surroundings of the target compound causes its precipitation in the form of nano- or microcrystal dispersion.[3−6] Large-scale synthesis is limited by the solubility of the target compound in the good solvent. Moreover, the heterogeneous environment of this method makes it difficult to precisely control the complicated nucleation process in the initial stages and the subsequent fast growth.[4] Consequently, the broad distribution in both the size and the shape of the ONPs generated using this method prevent them from acting as building blocks for further self-organization.

Many chemical reaction syntheses for organic compounds are conducted at room temperature in the solution phase in which the reactant precursors are well dissolved and the target product is generated as a precipitate. The homogeneous solution phase makes it possible to continuously tune the supersaturation during precipitation of the target product.[14a,20] We expect that the adjustment of the reaction conditions will pave the way for manipulating the precipitation process of the target product and thus the resulted nanoparticles. In this study, by employing the colloid chemical reaction method, we demonstrate for the first time the preparation of ONPs composed of perylene molecules (PeNPs) based on the reduction of perylene perchlorate by Br^- anions[21] in the presence of cetyl trimethyl ammonium bromide (CTA^+Br^-) in acetonitrile. We found that the homogeneous solution phase of this method provides several advantages, including the facile separation of the nucleation and growth stages and an easier controllability of the growth parameters by changing certain variables, such as monomer concentration (much higher than that in the reprecipitation method) and method of injection. The large-scale synthesis of PeNPs ranging from 25 to 90 nm with a polydispersity of $<10\%$ is achieved. Furthermore, the hierarchical self-organization of 25-nm PeNP building blocks is observed to form nanobelts and/or square nanorods. Spectroscopic results reveal that the PeNPs and their self-assemblies present different optical properties from those of the monomers and bulk powder. The size dependence is evidenced by a transition from Y-type excimers to E-type excimers as the size of the PeNPs increases from 25 to 90 nm. As 25-nm PeNPs organize into nanobelts or square nanorods, development of collective phenomena is observed. Our very recent results indicate that this colloid chemical-reaction method can also be applied to other organic compounds.

Results and Discussion

In our experiments, first a precursor of perylene perchlorate is produced via reaction 1[21]

$$2Pe + 2Ag^+ClO_4^- + I_2 \rightarrow 2Pe^+ClO_4^- + 2Ag^+I^- \quad (1)$$

where Pe is perylene. Then varying quantities of 10 mM cetyl trimethyl ammonium bromide (CTA^+Br^-) solution in acetonitrile are injected into 1 mL of 4.0 mM perylene perchlorate in acetonitrile. Following reduction of Pe^+ by Br^- via reaction 2[21]

$$2Pe^+ClO_4^- + 2CTA^+Br^- \rightarrow 2Pe + Br_2 + 2CTA^+ClO_4^- \quad (2)$$

the newly generated perylene molecules might undergo nucleation and growth, giving rise to PeNPs.[20c] (Production of perylene via reaction 2 has been evidenced by ^1H NMR and ESI-MS results, as shown in Figure S1 in the Supporting Information. The reaction yield is nearly 100% with respect to the amount of CTA^+Br^- added into the system by titration of

(9) (a) Hu, D.; Yu, J.; Padmanaban, G.; Ramakrishnan, S.; Barbara, P. F. *Nano Lett.* **2002**, *2*, 1121. (b) Patra, A.; Hebalkar, N.; Sreedhar, B.; Sarkar, M.; Samanta, A.; Radhakrishnan, T. P. *Small* **2006**, *2*, 650.
(10) (a) McNeill, J. D.; O'Connor, D. B.; Barbara, P. F. *J. Chem. Phys.* **2000**, *112*, 7811. (b) Schwartz, B. J. *Annu. Rev. Phys. Chem.* **2003**, *54*, 141.
(11) Alivisatos, A. P. *Science* **1996**, *271*, 933. (b) Halperin, W. P. *Rev. Mod. Phys.* **1986**, *58*, 533.
(12) Pope, M.; Swenberg, C. E. *Electronic Processes in Organic Crystals*; Oxford Univ. Press: Oxford, 1982.
(13) Silinsh, E. A. *Organic Molecular Crystals: Their Electronic States*; Springer-Verlag: Berlin, 1980.
(14) (a) Murray, C. B.; Kagan, C. R.; Bawendi, M. G. *Annu. Rev. Mater. Sci.* **2000**, *30*, 545. (b) Murray, C. B.; Kagan, C. R.; Bawendi, M. G. *Science* **1995**, *270*, 1335. (c) Heitmann, D.; Kotthaus, J. P. *Phys. Today* **1993**, *46*, 56.
(15) (a) Zhao, Y. S.; Di, C. A.; Yang, W. S.; Yu, G.; Liu, Y. Q.; Yao, J. N. *Adv. Funct. Mater.* **2006**, *16*, 1981. (b) Zhao, L. Y.; Yang, W. S.; Luo, Y.; Zhai, T. Y.; Zhang, G. J.; Yao, J. N. *Chem. Eur. J.* **2005**, *11*, 3773.
(16) (a) Ibanez, A.; Maximov, S.; Guiu, A.; Chaillout, C.; Baldeck, P. L. *Adv. Mater.* **1998**, *10*, 1540. (b) Sanz, N.; Gaillot, A.-C.; Usson, Y.; Baldeck, P. L.; Ibanez, A. *J. Mater. Chem.* **2000**, *10*, 2723−2726. (c) Sanz, N.; Wang, I.; Zaccaro, J.; Beaugnon, E.; Baldeck, P. L.; Ibanez, A. *Adv. Funct. Mater.* **2002**, *12*, 352−358.
(17) (a) Gong, X. C.; Milic, T.; Xu, C.; Batteas, J. D.; Drain, C. M. *J. Am. Chem. Soc.* **2002**, *124*, 14290. (b) Balakrishnan, K.; Datar, A.; Zhang, W.; Yang, X.; Naddo, T.; Huang, J.; Zuo, J.; Yen, M.; Moore, J. S.; Zang, L. *J. Am. Chem. Soc.* **2006**, *128*, 6576.
(18) (a) Liu, H. B.; Li, Y. L.; Xiao, S. Q.; Gan, H. Y.; Jiu, T. G.; Li, H. M.; Jiang, L.; Zhu, D. B.; Yu, D. P.; Xiang, B.; Chen, Y. F. *J. Am. Chem. Soc.* **2003**, *125*, 10794. (b) Jang, J.; Oh, J. H. *Adv. Mater.* **2003**, *15*, 977.
(19) Tamaki, Y.; Asahi, T.; Masuhara, H. *J. Phys. Chem. A* **2002**, *106*, 2135.
(20) (a) Peng, Z. A.; Peng, X. G. *J. Am. Chem. Soc.* **2002**, *123*, 1389. (b) Peng, Z. A.; Peng, X. G. *J. Am. Chem. Soc.* **2001**, *123*, 183. (c) LaMer, V. K.; Dinegar, R. H. *J. Am. Chem. Soc.* **1950**, *72*, 4847.
(21) Ristagno, C. V.; Shine, H. J. *J. Org. Chem.* **1971**, *36*, 4050.

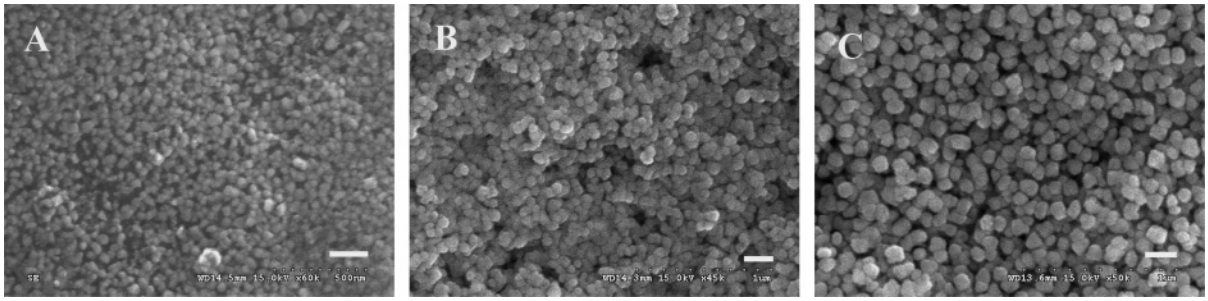

Figure 1. Typical FESEM images of quasi-spherical PeNPs with a size of (A) ~25 nm at $N = 0.3$, (B) ~60 nm at $N = 0.6$ fabricated by the droplet injection of CTA^+Br^-, and (C) ~90 nm at about $N = 1.0$ fabricated by the single injection of CTA^+Br^-. All scale bars are 200 nm.

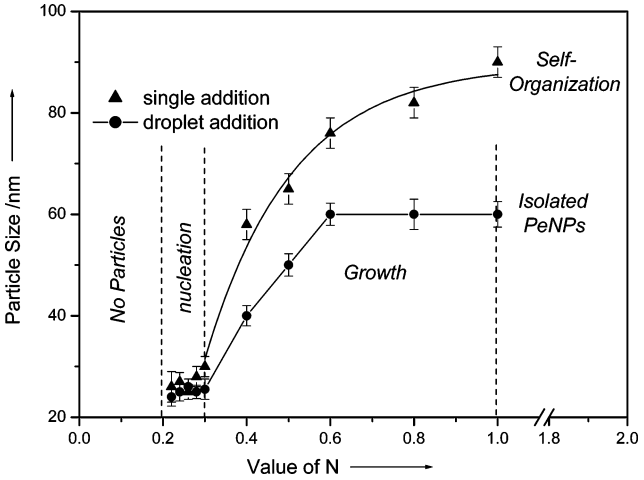

Figure 2. Sizes of PeNPs obtained by droplet (circle) and single (triangle) injections of CTA^+Br^- at different values of *N*.

the remaining precursors of perylene perchlorate.) By changing the quantity of 10 mM CTA^+Br^- solution, the molar ratio between the reductant and perylene perchlorate, i.e., $N = N(CTA^+Br^-)/N(Pe^+ClO_4^-)$, is systematically tuned. Since a different amount of perylene molecules is produced by reaction 2 at different values of *N*, the size of the PeNPs can be readily controlled. At the same value of *N* we found that the methods of injection, i.e., the single and/or droplet injection methods, also influence the size of the PeNPs. Both precursors, CTA^+Br^- and perylene perchlorate, have good solubility in acetonitrile. In our experiments large-scale synthesis of PeNPs ranging from 25 to 90 nm has been achieved. Some of their typical FESEM images are shown in Figure 1 in which the mean sizes are 25, 60, and 90 nm. (FESEM images recorded at low magnification are shown in Figures S2, S3, and S4 for PeNPs with a mean size of 25, 60, and 90 nm, respectively.) It can be seen from Figure 1 that the PeNPs obtained in all cases are quasi-spherical, showing clear boundaries, and are nearly monodisperse with a size distribution <10%.

Figure 2 summarizes the sizes of PeNPs obtained by droplet (circle) and single (triangle) injections at different values of *N*. Three distinctive stages are identified in the range of $0 \le N \le 1.0$. (i) No particles are detectable if $N < 0.2$. (ii) Primary particles are formed with an almost constant size of ~25 nm between $N = 0.2$ and 0.3. (iii) Growth on the primary particles leads to an increase in the size of the PeNPs upon increasing the value of *N* from 0.3 to 1.0. Similar behaviors are observed during the nucleation stage under conditions of $N < 0.3$ for both droplet and single injection methods. However, the growth behaviors are quite different when different injection methods are employed. In the case of the droplet injection method, the size of the PeNPs increases with increasing *N* from 0.3 to 0.6 and then maintains a constant value of ~ 60 nm at $N \ge 0.6$. In the case of the single injection method, the size of the PeNPs increases over the entire range of $0.3 \le N \le 1.0$ and is always larger than that obtained by droplet injection at the same *N*. Moreover, the size distribution of PeNPs obtained by the single injection method, ~10%, is slightly larger than that obtained by droplet injection, 5−8%.

Under conditions of $N > 1.0$, the amount of CTA^+Br^- is excessive on the basis of the stoichiometric relationship in reaction 2. The droplet injection method still produces isolated PeNPs with a size similar to that obtained at $N = 1.0$ since no more perylene molecules can be produced for the growth of PeNPs. In contrast, the single-injection method under conditions of $N > 1.0$ produces not only isolated PeNPs but also belt-like nanostructures (see Figure 3A, $N = 1.2$). Figure 3C shows that isolated PeNPs have a mean size of 90 nm, similar to that obtained by the single-injection method at $N = 1.0$. Figure 3B reveals that monolayered nanobelts, i.e., nanosheets, are factually composed of PeNPs of ~25 nm in a line-by-line arrangement. The width of the nanosheet is around 400 ± 50 nm, and the length amounts to several tens or hundreds of micrometers. The two intermediate states of Figure 3D and E, observed occasionally using samples with $1.0 < N < 1.2$, shield more light on formation of nanosheets. Figure 3D shows the appearance of nanowires of 25 nm in diameter out of a large volume of 25-nm PeNPs, while Figure 3E shows formation of a nanosheet by the close attachment of nanowires. These observations suggest that 25-nm PeNPs are building blocks for the self-organization of nanowires, which themselves can further undergo a line-by-line self-organization to form nanosheets (see more evidence in Figure S5). Thick nanobelts are formed with increasing the value of *N* to 1.4, as shown in Figure 3F; meanwhile, the amount of isolated 90-nm PeNPs drops considerably. A layer-by-layer self-organization process can be identified from Figure S6A in which a thinner nanosheet is found to peel off from a thicker nanobelt. It can be seen from Figure S6B that the match of the width of nanosheets is important in the layer-by-layer self-organization. Under conditions of $N \ge 2.0$, square nanorods are observed (Figure 3G, $N = 2.0$) while the isolated 90-nm PeNPs vanish completely. The white circle in Figure 3G marks a defect where the top and bottom layers remain after losing the middle part, confirming the layer-by-layer self-organization mechanism. The high-magnification image of Figure 3H clearly indicates that nanorods are also made up from 25-nm PeNPs, and the cross-section of nanorods is square-shaped with sides of length ≈ 400 nm. It is

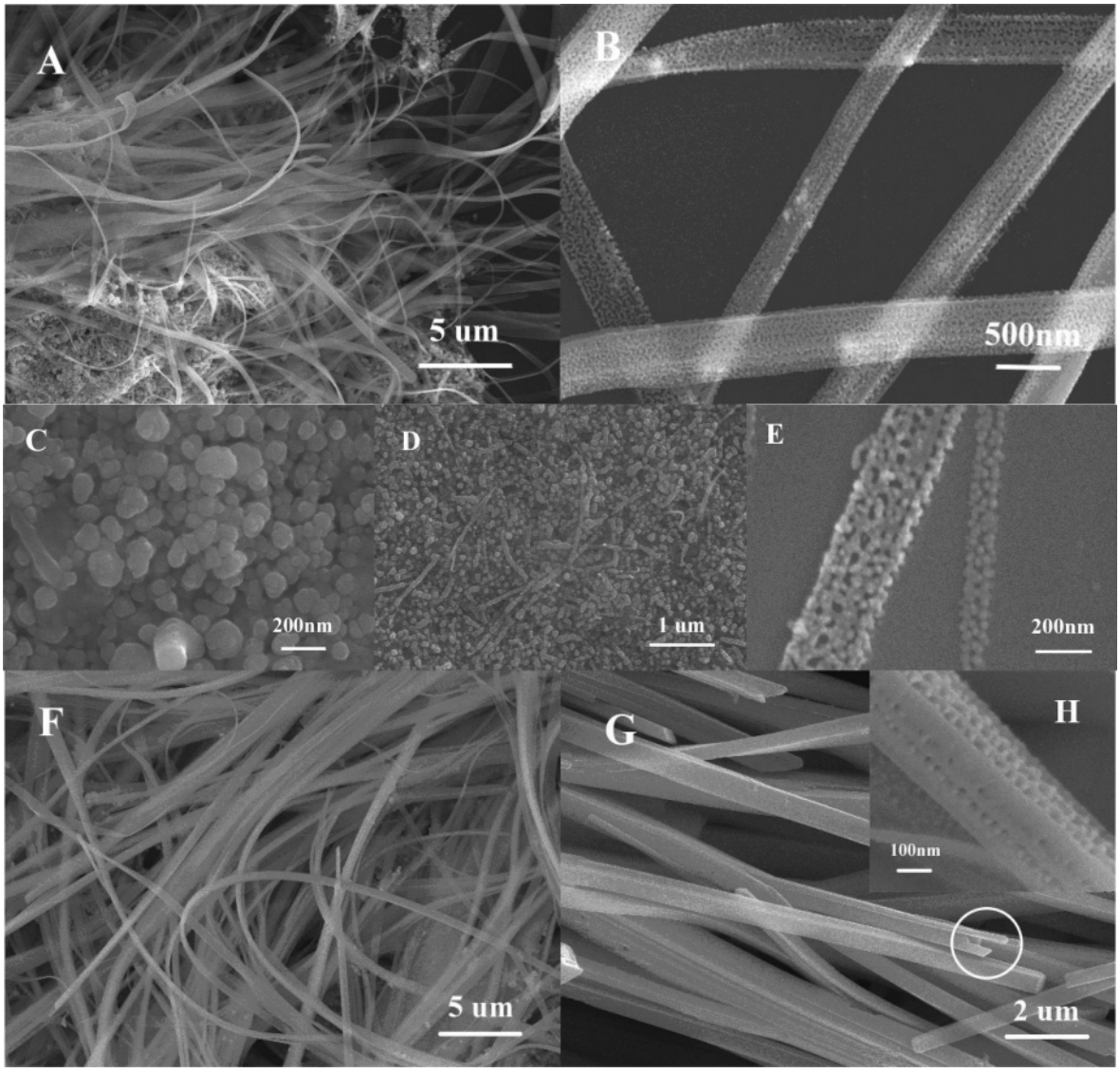

Figure 3. Self-organization of 25-nm PeNPs observed by employing the single injection of CTA^+Br^- at $N > 1.0$. (A−C) $N = 1.2$. (B and C) High-magnification images showing nanosheets and isolated nanoparticles, respectively. (D and E) $N = 1.0-1.2$; intermediate states observed occasionally. (F) $N = 1.4$; nanobelts. (G and H) $N = 2.0$; square nanorods. (H) High-magnification image from G; the white circle in G shows a defect. See text for details.

the match of the width of nanosheets required by the layer-by-layer self-organization that uniforms the nanorods into symmetrical square shape.

Tetrabutylammonium bromide (TBA^+Br^-) was also employed as the reducing agent in reaction 2 for the preparation of PeNPs. Under the conditions of $N < 1.0$, the behavior of the size of PeNPs versus N is quite similar to that observed in Figure 2. However, the PeNPs obtained using TBA^+Br^- are more irregular in shape (see Figure S4) with a broad size distribution. Moreover, aggregation of PeNPs obtained using TBA^+Br^- becomes a serious problem (see Figure S7). Note that Br^- is the actual reducing agent for reaction 2 in both cases.[21] Therefore, the CTA^+ molecules might form a protective layer around the as-prepared PeNPs, serving as colloid stabilizers. Most importantly, self-organization of PeNPs into ordered structures is not observed when TBA^+Br^- is used, irrespective of the value of N or the method of injection employed.

It is known that rod-like CTA^+Br^- micelles in the aqueous phase are widely used as templates in the synthesis of one-dimensional nanomaterials, including both inorganic[22,23] and organic[6d] species. The hydrophobic core of CTA^+ micelles provides a unique environment for the nucleation of hydrophobic materials, and the rod-like micelles serve as templates to direct the growth of these materials. In these cases, the final structure can be understood as a core/shell structure in which the continuum target compounds are located in the central core surrounded by a protective layer of CTA^+ molecules. However, Figure 3 presents hierarchical self-organization processes in which the separated 25-nm PeNPs represent building blocks.

Formation of micelle-like structures of CTA^+Br^- in nonaqueous solvents, such as acetonitrile, has received far less attention than the related phenomena in water.[24] The conductivity of CTA^+Br^- solution versus its concentration in acetonitrile

(22) (a) Jana, N. R.; Murphy, C. J. *Chem. Commun.* **2001**, 617. (b) Murphy, C. J.; Jana, N. R. *Adv. Mater.* **2002**, *14*, 80.
(23) (a) Yu, Y. Y.; Chang, S. S.; Lee, C. L.; Wang, C. R. C. *J. Phys. Chem. B* **1997**, *101*, 6661. (b) Link, S.; Mohamed, M. B.; El-Sayed, M. A. *J. Phys. Chem. B* **1999**, *103*, 3073.
(24) Myers, D. *Surfactant Science and Technology*, 2nd ed.; VCH: New York, 1992.

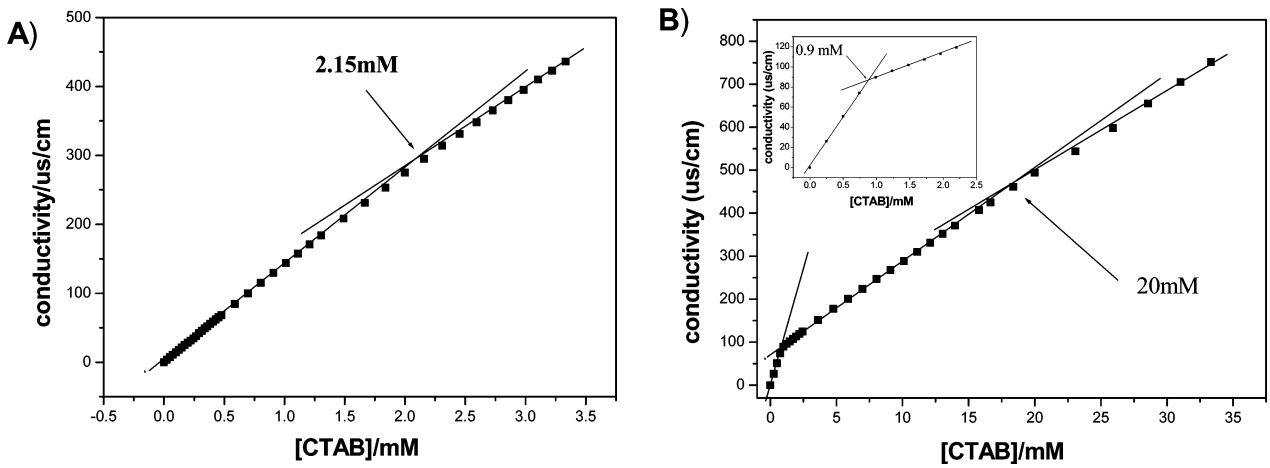

Figure 4. Changes in conductivity of CTA^+Br^- with respect to concentration in (A) acetonitrile and (B) water. The first and second critical micelle concentrations (CMC) of CTA^+Br^- in water are observed to be about 0.9 and 20 mM (B), respectively, which are consistent with literature data. The flex point at 2.15 mM in acetonitrile (A) suggests a transition between CTA^+Br^- monomers and micelle-like structures.

Table 1. Size of Isolated PeNPs and Self-Organization of 25-nm PeNPs under Different Experimental Conditions

$V(CTA^+Br^-, mL)$[a]	0.12	0.24	0.40	0.48	0.56	0.80
$C\ (CTA^+Br^-, mM)$[b]	1.07	1.94	2.85	3.24	3.59	4.44
N[c]	0.3	0.6	1.0	1.2	1.4	2.0
droplet injection[a]	~25 nm	~60 nm	~60 nm	~60 nm	~60 nm	~60 nm
single injection[a]	~25 nm	~76 nm	~90 nm	self-organization of 25-nm PeNPs		

[a] The different volume of 10 mM CTA^+Br^- was added into 1 mL of 4 mM perylene perchlorate in acetonitrile. [b] Final concentration of CTA^+Br^- in the colloidal suspensions of PeNPs, C = 10 mM × V mL/(1.0 mL + V mL) [c] $N = N(CTA^+Br^-)/N(Pe^+ClO_4^-)$ = (10 mM × V mL)/(1 mM × 4 mL).

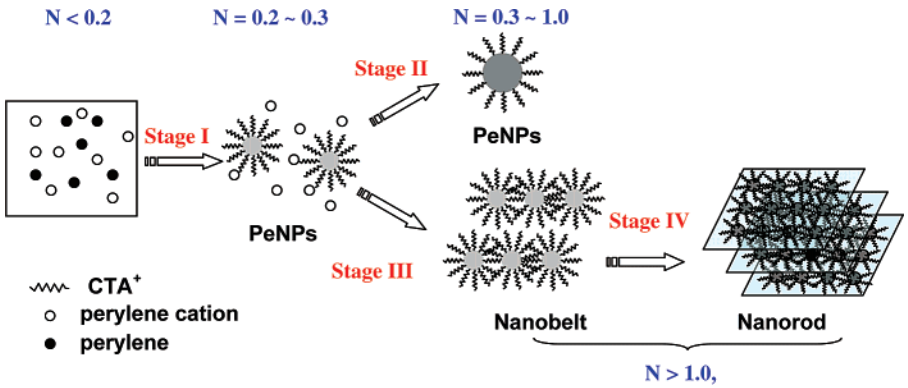

Figure 5. Schematic illustration representing formation of quasi-spherical PeNPs (upper path including stage I and stage II) and hierarchical self-organization of 25-nm PeNPs into nanobelts (lower path including Stages I, III, and IV): stage I, Nucleation; stage II, Growth; stages III and IV, 1D to 3D organization. See text for details.

reveals a flex point at 2.15 mM (see Figure 4A). A parallel experiment was also carried out in the aqueous phase. The observed flex points at 0.9 and 20 mM correspond well to the first and second critical micelle concentrations of CTA^+Br^- in water (see Figure 4B).[25] Dynamic light scattering (DLS) measurements of 3.0 mM CTA^+Br^- in water present a single size distribution centered at 7.9 nm, indicating formation of spherical micelles in the aqueous phase.[25a] However, DLS measurements of 3.0 mM CTA^+Br^- in acetonitrile yield multiple distributions varying randomly from several hundreds to several thousands of nanometers. It is reasonable that CTA^+ molecules may form complicated aggregates in acetonitrile, for example, rod-like or lamellar micelles,[24] if the concentration of CTA^+ is above 2.15 mM.

On the basis of the above observations, we summarized the experimental results under different experimental conditions in Table 1 and proposed a possible mechanism in Figure 5 for formation of PeNPs (upper path) as well as self-organization of 25-nm PeNPs (lower path). Under conditions of $N < 0.2$, the concentration of perylene molecules produced through reaction 2 is not enough to initiate nucleation. Between N = 0.2 and 0.3, however, it reaches the nucleation threshold. A nucleation burst generates primary PeNPs with a mean size of ~25 nm.[20c] This is a diffusion/reaction/nucleation-controlled process (stage I in Figure 5) and so is not influenced by the various methods of injection. Once primary PeNPs form, CTA^+ molecules can attach to them through hydrophobic interactions between the alkyl chains of CTA^+ and perylene, forming a protective layer (see left second picture in Figure 5). Note that the primary PeNPs and perylene cations remaining in the system are separated from each other because of electrostatic repulsive

(25) (a) Imae, T.; Kamiya, R.; Ikeda, S. *J. Colloid Interface Sci.* **1985**, *108*, 215. (b) Shikata, T.; Hirata, H.; Kotaka, T. *Langmuir* **1988**, *4*, 354. (c) Lianos, P.; Lang, J.; Strazielle, C.; Zana, R. *J. Phys. Chem.* **1982**, *86*, 1019.

interactions. By adding further CTA^+Br^- over $N = 0.3$, more perylene molecules are released by reaction 2 slowly and smoothly into the solution phase. As long as the consumption of feedstock by the growing PeNPs is not exceeded by the rate of perylene production, no new nuclei form. In other words, stage I of the nucleation process is separated from stage II of the growth process during formation of PeNPs (see Figure 5). The amount of perylene produced via reaction 2 increases with increasing N in the range of $0.3 \leq N \leq 1.0$; thus, the size of the PeNPs can be readily controlled. Since the instant concentration of perylene (supersaturation) is high when the single-injection method is employed, the growth rate of the primary 25-nm PeNPs is fast.[14a,20c] This is why both the size and the size distribution of PeNPs obtained by the single-injection method are larger than those obtained by the droplet injection method at the same value of N. As mentioned above, the size of the PeNPs obtained by the droplet injection method maintains a constant value of 60 nm above $N = 0.6$ at which the concentration of CTA^+ is close to 2.15 mM, as shown in Table 1. Therefore, this might be due to formation of aggregate structures of CTA^+ in the system. In any event, it is the separation between the nucleation and growth stages that improves the monodispersity of as-prepared PeNPs < 10%.

Under the conditions of $N > 1.0$, 60-nm PeNPs are already formed in the case of the droplet injection method. However, the situation is entirely different when the single-injection method is employed (stages III and IV in Figure 5). (i) A large amount of primary 25-nm PeNPs can be generated instantly prior to the growth process. This provides possible driving forces (interfacial energy) for self-organization of the 25-nm PeNPs due to the tendency of the system to try to minimize the free energy.[26] (ii) As above-mentioned, CTA^+ molecules can form a protective layer around PeNPs. Under high concentration of 25-nm PeNPs in the colloidal suspension, the surface-bound CTA^+ molecules can also assist in drawing the PeNPs closer to share a common layer of counterions or through the inner digitation of CATB tails from neighboring nanoparticles.[27] (iii) Since the concentration of CTA^+ in the samples with $N > 1.0$ is greater than 2.15 mM (see Table 1), the rod-like or lamellar micelle structures in the stock solution will exist when the single-injection method is employed. The rod-like micelles can induce self-organization of 25-nm primary PeNPs into nanowires.[6d] Furthermore, the lamellar micelles already present in solution or induced by replacement of the Br^- counter ions by ClO_4^- [28] serve as templates for self-organization of nanowires into nanobelts. Growth and self-organization of 25-nm PeNPs are competitive processes in the range of $1.0 < N < 2.0$. Under the conditions of $N \geq 2.0$, the latter process becomes the dominant pathway and only square nanorods are observed.

The spectroscopic studies, when correlated with the FESEM observations, further clarify formation of spherical PeNPs with different sizes as well as confirm the hierarchical self-organization of 25-nm PeNPs into nanobelts and square nanorods. In Figure 6, spectra m and p correspond to monomers in dilute solution and bulk powder, respectively. It can be seen from Figure 6 that PeNPs and their self-assemblies (colored spectra)

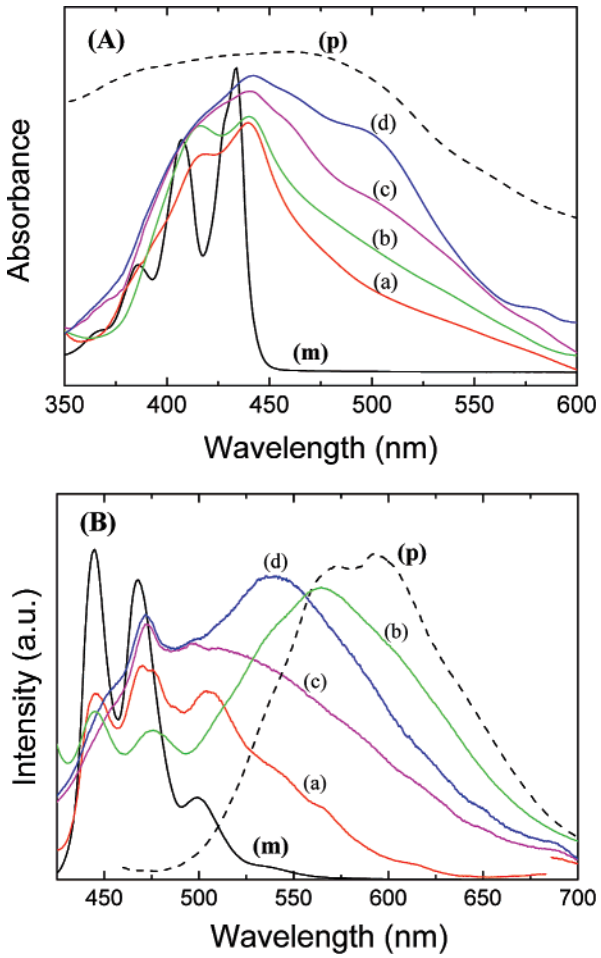

Figure 6. Absorption (A) and emission (B) spectra of samples prepared by the single injection of CTA^+Br^- at different values of N: (a) spherical PeNPs (25 nm) at $N = 0.3$, (b) spherical PeNPs (90 nm) at $N = 1.0$, (c) nanobelts at $N = 1.4$, and (d) square nanorods at $N = 2.0$. Spectra m and p are recorded for monomers in 1.0×10^{-5} M perylene/acetonitrile solution and bulk powder, respectively.

present different optical properties from those of the monomers and bulk powder. Figure 6A is the diffuse reflectance absorption spectra of nanoparticle samples that have been filtered on the surface of an alumina membrane. The appearance of a new peak in spectra a−d around 500 nm is ascribed to aggregate states and an indication of formation of nanoparticles.[1b] Meanwhile, the absorption bands between 350 and 450 nm corresponding to the molecular states in spectra a−d is slightly red-shifted from that in the monomer spectrum of m.

The emission spectrum a in Figure 6B observed for 25-nm PeNPs is dominated by transitions from the molecular states between 375 and 525 nm together with weak emissions at 535, 570, and 615 nm, which are attributed to the aggregate states. The emission spectrum p of the bulk powder presents peaks at 570 and 595 nm which are typical emissions associated with the so-called E-type excimer, i.e., a single-center sandwich or card-packed-type excimer.[29−31] Therefore, the emission features of 25-nm PeNPs at 570 and 615 nm are assigned to E-type excimers, while that at 535 nm is assigned to a Y-type excimer,

(26) Cross, M. C.; Hohenberg, P. C. *Rev. Mod. Phys*. **1993**, *65*, 851.
(27) (a) Wang, Z. L. *J. Phys. Chem. B* **2000**, *104*, 1153. (b) Sau, T. K.; Murphy, C. J. *Langmuir* **2005**, *21*, 2923.
(28) Zhang, X. T.; Zhang, J.; Liu, Z. F.; Robinson, C. *Chem. Commun.* **2004**, *16*, 1852.
(29) Tanaka, J. *Bull. Chem. Soc. Jpn.* **1963**, *36*, 1237.
(30) Weiss, D.; Kietzmann, R.; Mahrt, J.; Tufts, B.; Storck, W.; Willing, F. *J. Phys. Chem.* **1992**, *96*, 5320.
(31) (a) Akimoto, S.; Ohmori, A.; Yamazaki, I. *J. Phys. Chem. B* **1997**, *101*, 3753. (b) Liu, J. S.; Wang, L.; Gao, F.; Li, Y. X.; Wei, Y. *Anal. Bioanal. Chem*. **2003**, *377*, 346.

i.e., a two-center or partial overlapping excimer.[32] Remarkably, Figure 6B elucidates two different kinds of trends in the development of the emission properties if the 25-nm PeNPs are considered as a starting point. (i) As the size of the PeNPs increases from 25 to 90 nm, the emission from the aggregate states at longer wavelengths becomes dominant and shifts from a Y-type excimer at 535 nm (spectrum a) to a E-type excimer at 570 nm (spectrum b). Perylene microcrystals in the range from 300 nm to 1 μm, prepared by the reprecipitation method, have been reported to show size-dependent optical properties.[33,34] The particle size dependence of the emission maxima is explained in terms of lattice softening,[1b,33,34] which makes the intermolecular interactions weaker and modifies the energy level of the excimer state (only E-type in ref 33). Our results add new data for the range below 100 nm. The quasi-spherical shape of the PeNPs (<100 nm) suggests that these particles are amorphous. Lattice softening is therefore no longer an appropriate term. However, the intermolecular interactions might still decrease with decreasing particle size since the surface-to-volume ratio increases significantly in this range. The loose intermolecular environment allows coexistence of both E-type and Y-type excimers in PeNPs, the percentages of which are dependent on the particle size. (ii) It can also be seen from Figure 6 that the absorption at 500 nm (Figure 6A) and the luminescence at 535 nm (Figure 6B) in the self-organization samples (spectra c and d) become stronger than those of the 25-nm PeNP building blocks (spectrum a), a result which cannot be explained by the size-dependence theory.[1b,33,34] As shown in Figure 3, the nanobelts and square nanorods are glassy solids formed by the building blocks of 25-nm PeNPs. The width of these nanobelts and square nanorods is 400 nm, while their length amounts to several micrometers. Though the size of the square nanorods is much larger than that of the 90-nm PeNPs, the emission maxima of the former (spectrum d) at 535 nm is still attributed to the Y-type excimers, different from the emission maxima of the latter at 570 nm attributed to the E-type excimers (spectrum b). The enhancement of the oscillator strength for Y-type excimers upon assembling 25-nm PeNPs into glassy solids is due to the fact that collective phenomena develop as proximal 25-nm PeNPs interact. This opens up the possibilities of fabricating solid-state materials with novel physical properties.

Conclusion

In summary, we demonstrate that the colloid chemical method in the solution phase can be applied to the preparation of perylene nanoparticles. The homogeneous solution phase of this method provides several advantages, including facile separation of the nucleation and growth stages and an easier controllability of the growth parameters, such as the monomer concentration and method of injection. The large-scale synthesis of PeNPs ranging from 25 to 90 nm is achieved with a size distribution (<10%) that is improved by formation of a protective layer of CTA^+ around the PeNPs. The three-dimensional hierarchical self-organization of PeNPs with size ~25 nm is observed to form nanobelts and square nanorods, possibly templated by the CTA^+ lamellar micelle structures in acetonitrile. Spectroscopic results reveal two kinds of trends in the development of the optical properties of perylene as they evolve from the molecular to the bulk phase in the nanometer range. The size dependence is characterized by a switch from formation of Y-type excimers to E-type excimers as the size of the PeNPs increases from 25 to 90 nm. As the 25-nm PeNPs organize into nanobelts or square nanorods, the oscillator strength of the Y-type excimers is relatively enhanced. That is, collective phenomena develop as proximal particles interact in the glassy solids. Our results suggest that the colloidal chemical reaction method and subsequent self-organization might be useful in the fabrication of highly ordered organic nanomaterials.

Experimental Section

Materials. Compounds perylene and silver perchlorate were purchased from Aldrich chemical Co. Iodine (A.R.), cetyl trimethyl ammonium bromide (CTA^+Br^-, A.R.), and tetrabutylammonium bromide (TBA^+Br^-) were obtained from Beijing Chemical Co., China. Solvents dichloromethane (HPLC grade) and anhydrous acetonitrile (water < 0.001%) were purchased from Tianjin Chemical Co. and Aldrich, respectively. Ultrapure water with a resistivity of 18.2 MΩ was produced using a Milli-Q apparatus (Millipore). Alumina membranes with a pore size of 20 nm and polytetrafluoroethylene filters (PTFE, Puradisc 25 TF, 0.1 μm) were bought from Whatman International Ltd.

Preparation and Analysis of PeNPs. *(A) Preparation of Perylene Perchlorate.*[21] A solution of 1 mmol of dry silver perchlorate in a minimum amount of anhydrous acetonitrile was added into a 100 mL solution of 10 mM perylene in anhydrous dichloromethane with stirring. To this mixture was added a solution of 0.5 mmol of iodine in a minimum amount of anhydrous dichloromethane. A dark precipitate formed immediately. After stirring for 15 min, the mixture was separated by centrifuging at 12 000 rpm. Relying on the difference in solubility between silver iodide and perylene perchlorate in acetonitrile, perylene perchlorate is separated from the admixture and dried under vacuum at room temperature.

(B) Preparation of PeNPs. Varying quantities of 10 mM CTA^+Br^- or TBA^+Br^- solution in anhydrous acetonitrile were added into 1 mL of 4 mM perylene perchlorate in anhydrous acetonitrile under vigorous stirring. After injection, the aubergine solution gradually turned yellow, and the colloidal suspension of PeNPs was obtained. The nanoparticle samples collected on the surface of an alumina membrane were dried under vacuum, washed twice with ultrapure water, and finally dried again under vacuum for further analysis. In our experiment the size of PeNPs was tuned by both the methods of injection, i.e., quick single injection or droplet addition (25 μL/drop, 1 drop/30 s), and the molar ratio of the reducing agent to the perylene perchlorate, i.e., $N = N(CTA^+Br^-)/N(Pe^+ClO_4^-)$. Experimental results under different experimental conditions are summarized in Table 1.

(C) Analysis. First, the sample on the alumina membrane was analyzed by ^1H NMR (400 MHz, Bruker ARX 400 Spectrometer) and ESI-MS (LC-MS 1020), and the details can be found in the Supporting Information (see Figure S1). The morphology and size of the sample were examined by field emission scanning electron microscopy (FESEM, Hitachi S-4300). The optical properties of the sample were investigated by steady-state fluorescent (Hitachi F-4500) and diffuse reflectance UV−vis absorption spectroscopies (Lambda 35 1.27 spectrometer), respectively. All samples remain stable after being kept at room temperature in air for several months according to a comparison the optical properties before and after. The quantum yield of perylene nanoparticles, which were redispersed into ultrapure water, was

(32) Xie, R. M.; Xiao, D. B.; Fu, H. B.; Ji, X. H.; Yang, W. S.; Yao, J. N. *New J. Chem.* **2001**, *25*, 1362.
(33) Oikawa, H.; Mitsui, T.; Onodera, T.; Kasai, H.; Nakanishi, H.; Sekiguchi, T. *Jpn. J. Appl. Phys.* **2003**, *42*, L111.
(34) (a) Kasai, H.; Kamatani, H.; Yoshikawa, Y.; Okada, S.; Oikawa, H.; Watanabe, A.; Itoh, O.; Nakanishi, H. *Chem. Lett.* **1997**, *26* (9), 1181. (b) Latterini, L.; Roscini, C.; Carlotti, B.; Aloisi, G. G.; Elisei, F. *Phys. Stat. Sol.* **2006**, *203*, 1470.

measured to be 0.09 at 298 K using the anthracene in ethanol as the standard (quantum yield, 0.27).[34b,35] (The mean deviation in the measurement of the quantum yield is 20%, largely owing to the Mie scattering of the colloidal suspensions.)

Acknowledgment. This work was supported by the National Natural Science Foundation of China (Nos. 90301010, 20373077, 20471062, 50573084, 90606004), the Chinese Academy of Sciences ("100 Talents" Program), and the National Research Fund for Fundamental Key Project 973 (2006CB806200). The authors thank Prof. Y. L. Wang in the same institute for her assistance in the measurement of CTA^+Br^- conductance.

Supporting Information Available: ^{1}H NMR (400 MHz) and EI-MS spectra of perylene from nanoparticle samples; FESEM images of perylene nanoparticles and their self-assemblies formed under different experimental conditions. This material is available free of charge via the Internet at http://pubs.acs.org.

JA068710D

(35) Eaton, D. F. Luminescence spectroscopy. In *Handbook of Organic Photochemistry*; Scaiano, J. C., Ed.; CRC Press; Boca Raton, 1989; Vol. 1.